Radiotherapy and Oncology 130 (2019) 121–131

Contents lists available at ScienceDirect

Radiotherapy and Oncology

journal homepage: www.thegreenjournal.com

Original article

Diffusion-weighted MRI and ADC versus FET-PET and GdT1w-MRI for gross tumor volume (GTV) delineation in re-irradiation of recurrent glioblastoma

Ilinca Popp [a,*], Stefan Bott [a], Michael Mix [b,i], Oliver Oehlke [a,1], Tanja Schimek-Jasch [a], Carsten Nieder [c,d], Ursula Nestle [a,i,1], Michael Bock [e], William T.C. Yuh [f], Philipp Tobias Meyer [b,i], Wolfgang A. Weber [g,j], Horst Urbach [h], Irina Mader [h,2], Anca-Ligia Grosu [a,i,2]

[a] Department of Radiation Oncology; [b] Department of Nuclear Medicine, Medical Center – University of Freiburg, Germany; [c] Department of Oncology and Palliative Medicine, Nordland Hospital, Bodø; [d] Department of Clinical Medicine, Faculty of Health Sciences, University of Tromsø, Norway; [e] Department of Radiology, Medical Physics, Medical Center – University of Freiburg, Germany; [f] University of Washington School of Medicine, Department of Radiology, Seattle, USA; [g] Department of Nuclear Medicine, Klinikum rechts der Isar, Technical University of Munich; [h] Department of Neuroradiology, Medical Center – University of Freiburg; [i] German Cancer Consortium (DKTK), Partner Site Freiburg; and [j] German Cancer Consortium (DKTK), Partner Site Munich, Germany

ARTICLE INFO

Article history:
Received 13 April 2018
Received in revised form 18 July 2018
Accepted 27 August 2018
Available online 12 September 2018

Keywords:
Diffusion weighted magnetic resonance imaging
Positron-emission tomography
Gross tumor volume delineation
Recurrent glioblastoma
Re-irradiation

ABSTRACT

Background and purpose: GTV definition for re-irradiation treatment planning in recurrent glioblastoma (rGBM) is usually based on contrast-enhanced MRI (GdT1w-MRI) and, for an increased specificity, on amino acid PET. Diffusion-weighted (DWI) MRI and ADC maps can reveal regions of high cellularity as surrogate for active tumor. The objective of this study was to compare the localization and quality of diffusion restriction foci (GTV-ADClow) with FET-PET (GTV-PET) and GdT1w-MRI (GTV-GdT1w-MRI).

Material and methods: We prospectively evaluated 41 patients, who received a fractionated stereotactic re-irradiation for rGBM. GTV-PET was generated automatically (tumor-to-background ratio 1.7–1.8) and manually customized. GTV-ADClow was manually defined based on DWI data (3D diffusion gradients, $b = 0$, 1000 s/mm^2) and parametric ADC maps. The localization of recurrence was correlated with initial GdT1w-MRI and PET data.

Results: In 30/41 patients, DWI-MRI showed areas with restricted diffusion (mean ADC-value 0.74 ± 0.22 mm^2/s). 66% of GTVs-ADClow were located outside the GdT1w-MRI volume and 76% outside increased FET uptake regions. Furthermore, GTVs-ADClow were only partially included in the high dose volume and received in mean 82% of the reference dose. An adjusted volume including GdT1w-MRI, PET-positive and restricted diffusion areas would imply a GTV increase of 48%. GTV-PET and GdT1w-MRI correlated better with the localization of re-recurrence in comparison to GTV-ADClow.

Conclusion: Unexpectedly, GTV-ADClow overlapped only partially with FET-PET and GdT1w-MRI in rGBM. Moreover, GTV-ADClow correlated poorly with later rGBM-recurrences. Seeing as a restricted diffusion is known to correlate with hypercellularity, this imaging discrepancy could only be further explained in histopathological studies.

 Radiotherapy and Oncology 130 (2019) 121–131

Re-irradiation of recurrent glioblastoma (rGBM) has been increasingly shown to be a well-tolerated therapeutic option, which may delay disease progression and improve survival [1,2]. However, re-irradiating brain tissue after having generally applied doses of 60 Gy in 30 fractions in the primary situation is a rather challenging approach in radiation oncology. Even if standard procedures have not yet been established, it is clear that reducing the re-irradiated volume to the absolute necessary, i.e. to the active tumor region, is of utmost importance for enhancing efficacy, while decreasing possible neurotoxicity. Consequently, efforts are undertaken to define optimal imaging methods of identifying real tumor extension for gross tumor volume (GTV) delineation and for confidently diagnosing progression in recurrent gliomas [3].

GBM, in particular, has a heterogeneous consistency and may entail different components, reflected also in its name. Necrotic, hemorrhagic or cystic areas and perilesional edema will exhibit different biological features, cell densities, cellular metabolisms and degrees of blood-brain-barrier (BBB) disruption. Furthermore,

* Corresponding author at: Department of Radiation Oncology, Medical Center University of Freiburg, Robert-Koch Str. 3, 79106 Freiburg, Germany.
E-mail address: ilinca.popp@uniklinik-freiburg.de (I. Popp).
[1] Present address: Department of Radiation Oncology, Kliniken Maria Hilf, Moenchengladbach, Germany.
[2] Equal contribution.

https://doi.org/10.1016/j.radonc.2018.08.019
0167-8140/

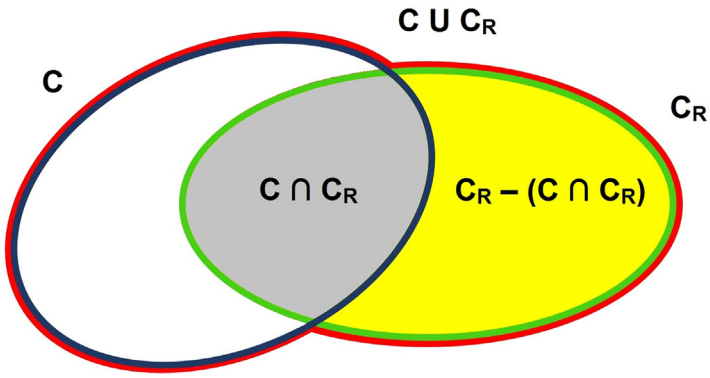

Overlap Volume (C_R, C)	C ∩ C_R	Optimum: C = C_R
Non-Overlap Volume (C_R, C)	C_R – (C ∩ C_R)	Optimum: 0
Union Volume (C_R, C)	C U C_R	Optimum: C = C_R
Common Delineated Volume (C_R, C)	CDV = (C ∩ C_R)/ C_R	Optimum: 1
Dice Similarity Coefficient (C_R, C)	DSC = 2x(C ∩ C_R)/(C + C_R)	Optimum: 1

Fig. 1. Schematic representation of measured parameters. Blue – C, the contour to be compared; green – CR, the reference contour; red – union volume; grey – overlap volume; yellow – non-overlap volume.

it is necessary to understand the biology of tumor recurrence after treatment in order to avoid confounding imaging results. Radiation and systemic therapy-induced early onset changes, such as pseudoprogression or pseudoresponse, and delayed onset transformations, including radiation necrosis, are variable and can often be incorrectly interpreted with anatomical contrast (Gadolinium) enhanced T1-weighted MRI (GdT1w-MRI) alone.

Contouring recurrent high-grade glioma foci based on GdT1w-MRI alone ensures a specificity of only 50% [4]. Biological imaging was shown to improve tumor detection and radiation treatment planning. Particularly, data on the additional use of amino acid (AA)-PET, such as L-[methyl-11C]methionine (MET)- or O-(2-[18F] fluoroethyl)-L-tyrosine (FET)-PET, illustrate a considerably higher specificity of 75–90%, due to a specific tracer uptake in tumor cells [5–10]. In previous studies we showed that GTVs defined according to GdT1w-MRI and AA-PET for re-irradiation may vary significantly [5,6,10]. To determine which of these two investigations is best for radiation treatment planning, further research is underway in form of the prospective phase II multicentric GLIAA trial [11]. Although the addition of FET-PET to the work-up panel and GTV delineation in rGBM has significantly improved the diagnostic accuracy [9], even this investigation may render false-positive results. Through passive influx in regions of disrupted BBB, tracer uptake may be seen in acute inflammatory conditions, hematomas, cerebral ischemia or marked radiation necrosis [12,13].

Diffusion-weighted (DWI) MRI is nowadays often an integral component of routine MRI investigations and has been perceived as a more affordable and commonly available alternative to AA-PET. Together with the corresponding apparent diffusion coefficient (ADC) maps, it illustrates restricted diffusion of water molecules in the cellular microenvironment. The degree of diffusion restriction correlates directly, while ADC values were shown to inversely correlate with increased tissue cellularity in various tumor entities, particularly in the brain [14–16]. Thus, areas of restricted diffusion may serve as a surrogate for active tumor tissue. The question was then raised whether these advanced MRI techniques could also help distinguish real tumor recurrence from benign changes [17]. Apart from offering information on tissue cellularity, DWI appears to be able of separating tumor from edema and differentiating cystic and necrotic tumor components, especially after correlation with ADC maps and anatomical MRI [18,19].

ADC and DWI-MRI are not currently used in the definition of GTVs – neither for re-irradiation, nor in the primary setting. The current study aims to establish whether GdT1w-MRI, FET-PET and DWI-MRI provide similar information on tumor extent and localization in rGBM and discuss the possible implementation of DWI-MRI in the GTV-delineation for re-irradiation.

Methods and materials

Study patients

41 patients (31 male, 10 female) with histologically confirmed rGBM scheduled for re-irradiation in the Department of Radiation Oncology, Medical Center-University of Freiburg, were prospectively enrolled (Pilot/GLIAA monocentric, prospective trial), in mean 17.1 months (±18, median 12.2, range 5.6–117.5 months) after the first irradiation. The median age was 58 years (range 35–77 years). All patients had an Eastern Cooperative Oncology Group (ECOG) performance status ≤ 1 and had previously undergone resection and adjuvant radiochemotherapy of their primary tumor with doses of 59.4–60 Gy in 33–30 fractions. The demographic and clinical characteristics of all patients are presented in Appendix A. The diagnosis of tumor recurrence was based on MRI, FET-PET and/or biopsy and confirmed in consensus in the Tumor Conference of the certified Neurooncological Center – Comprehensive Cancer Center Freiburg. The imaging (MRI, PET) protocol was identical. This additional analysis was approved by the local ethical committee and written informed consent was obtained from all patients[3].

Imaging

For re-irradiation treatment planning, patients were immobilized in supine position with a customized thermoplastic mask and underwent a planning PET/CT (Philips GEMINI TF Big Bore PET/CT) with 2-mm-thick slices in the Department of Nuclear Medicine. The investigation was performed using the AA-tracer FET. A

[3] This work has made the object of the doctoral dissertation of S. Bott "Integration der MRT-Diffusionsbildgebung in die Strahlentherapieplanung beim rezidivierenden Glioblastoma multiforme. [Integration of diffusion-weighted MRI in the radiation therapy planning of recurrent glioblastoma]", Freiburg University, Germany, 2017.

scan of 20 minutes duration was started 20 minutes after the intravenous injection of 200–300 MBq FET [11].

Each patient further received a routine multiparametric MRI in the Department of Neuroradiology. The cranial MRI was performed with a field magnitude of 1.5 Tesla, including axial T2 and fluid-attenuated inversion recovery (FLAIR) sequences, axial and 3D T1-weighted native and GdT1w-MRI. For the latter, following parameters were used: pulse repetition time (TR): 2200/2050 ms; echo time (TE) 3.02/2.15 ms; slice thickness 1 mm; voxel size $1 \times 1 \times 1$ mm. DWI was acquired for all patients by single-shot spin-echo echo-planar imaging and used for generating ADC maps. The employed parameters were: TR 4300/3700 ms; TE 102/100 ms; 23 slices of 5 mm thickness; voxel size $1.2 \times 1.2 \times 5$ mm; b-values 0 and 1000 s/mm^2. The diffusion-weighing was performed by means of a trace-weighted sequence type 3 (3 orthogonal directions). Follow-up MRIs were performed for each patient 6 weeks after re-irradiation and every 3 months thereafter.

GTV delineation

Separate planning volumes were delineated according to GdT1w-MRI and FET-PET in the iPlan Net radiotherapy planning software (Version 3.0.0, 2009 ©BrainLAB AG, Munich, Germany) as stipulated in the clinical trial protocol. The GTV-GdT1w-MRI was delineated exclusively based on the GdT1w-MRI image dataset and included any tumor-related contrast enhancement. For the delineation of PET volumes (GTV-PET), a tumor-to-background ratio of 1.7–1.8 was chosen. This led to the automatic generation of isocontours, which were then manually edited by experienced radiation oncologists in collaboration with nuclear medicine physicians in order to exclude anatomical boundaries and physiological uptake areas.

The clinical target volume (CTV) was defined by adding 3 mm in either direction respecting anatomical boundaries and expanded by 1–2 mm to the planning target volume (PTV) according to the tumor localization and type of mask used. The prescribed irradiation dose was in median 39 Gy (mean 38.59, range 30–46 Gy), 3 Gy/d (except one patient who received 2 Gy/d), 5x/week and was set to ensure coverage of at least 95% of the PTV [11]. The re-irradiation plan was based on GdT1w-MRI and/or FET-PET and best clinical practice (44% of patients both GdT1w-MRI and FET-PET, 29% GdT1w-MRI, 27% FET-PET).

For delineation of GTVs according to DWI-MRI/ADC maps (GTV-ADClow) and data assessment, MR-sequences were subsequently imported in the radiotherapy software Artiview^{TM} (Version 2.8.2, 2004 ©AQUILAB, Loos les Lille, France). An automated co-registration was performed and manually corrected.

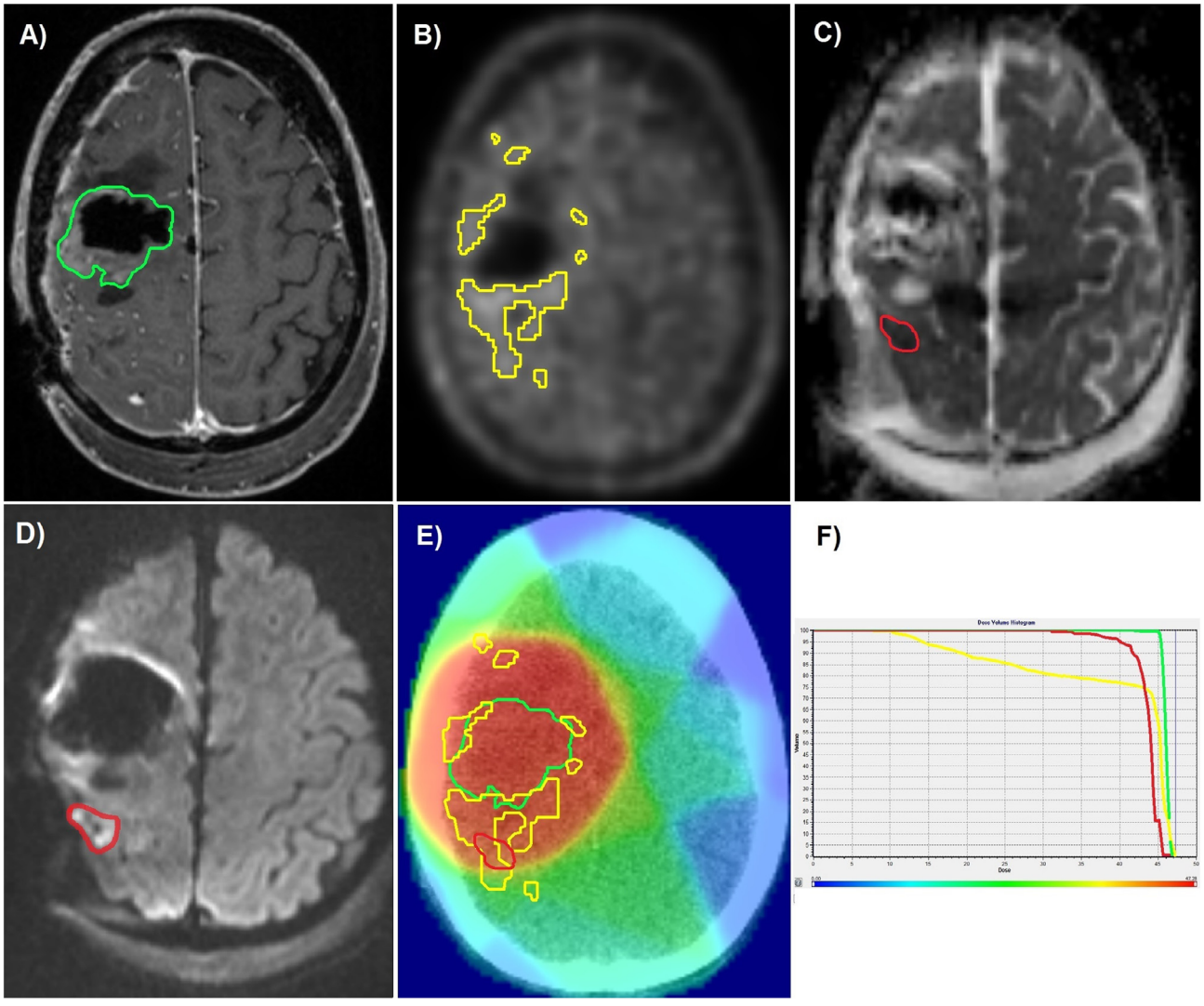

Fig. 2. Patient 30. A) Axial GdT1w-MRI, green: GTV-GdT1w-MRI. B) Axial FET-PET, yellow: GTV-PET. C) ADC map, red: GTV-ADClow, corresponding to a hyperintensity in D) DWI-MRI E) Illustration of all three volumes on planning CT as well as dose distribution and F) DVH of the treatment plan based on GdT1w-MRI with underdosage in both PET (yellow) and ADC (red) volumes.

GTVs-ADClow were outlined in the ADC maps together with experienced neuroradiologists. In order to best assess the regions of restricted diffusion, DWI, ADC maps, native and GdT1w-MRI sequences were simultaneously analyzed. Thus, the inclusion of areas with restricted diffusion that corresponded to non-tumor-related causes (such as hemorrhage, emboly, necrosis, gliosis) was minimized. The quantitative evaluation of restricted diffusion foci was performed by means of a Region-of-Interest (ROI) analysis. On every cross-section of the ADC map, free-hand ROIs were manually defined within the marked GTVs-ADClow around the diffusion restriction areas. The mean ADC-values of the ROIs were analyzed.

The first GdT1w-MRI images showing tumor progression after re-irradiation, confirmed either by serial MRIs (after corticosteroid therapy to exclude pseudoprogression), FET-PET and/or histology, were selected. Images were imported in Artiview™ (Version 2.8.2, 2004 ©AQUILAB, Loos les Lille, France), automatically co-registered and manually adjusted. Recurrence GTVs (GTV-R) were delineated including any tumor-related contrast enhancement on follow-up GdT1w-MRI.

For each patient, a comparative volumetric analysis of the GTVs was performed, calculating the overlap, non-overlap, union and the common delineated volumes (CDV), as well as the dice similarity coefficient (DSC), as illustrated in Fig. 1. Furthermore, the dose distribution in GTV-ADClow was assessed according to the plan used for re-irradiation. The evaluation involved measurement of various indices defined by the International Commission on Radiation Units and Measurements (ICRU) on dose-volume histograms (DVH) [20].

Statistical analysis

Data were analyzed using IBM SPSS Statistics software (Version 25.0, 2017 ©IBM Corp., Armonk, N.Y.) and explored both in a descriptive manner and by means of paired sample t-tests. To account for potential violations of normality, analyses were supplemented with their non-parametric equivalent (Wilcoxon matched pairs signed-rank test) whenever necessary. A Bonferroni-Holm correction for multiple testing was performed.

Results

The delineation of GTVs according to GdT1w-MRI and FET-PET/CT was performed successfully in all patients. Contouring the GTVs-ADClow was possible only in 30 of 41 patients, where DWI-MRI showed areas of restricted diffusion. These were quantitatively characterized by means of ROIs. At least one ROI was defined in each section plane of the GTVs-ADClow, with a maximum of 7 ROIs/patient. The mean ADC values within each ROI are presented in Appendix A. The mean ADC value across all ROIs was $0.74 \pm 0.22 \times 10^{-3}$ mm^2/s (median: 0.74×10^{-3} mm^2/s, range $0.25–1.44 \times 10^{-3}$ mm^2/s).

Volumetric analysis

The mean tumor volume measured according to GdT1w-MRI was 10.43 ± 9.34 ml (median volume 7.11 ml, range 0.87–48.27 ml). In comparison, GTV-ADClow was significantly smaller

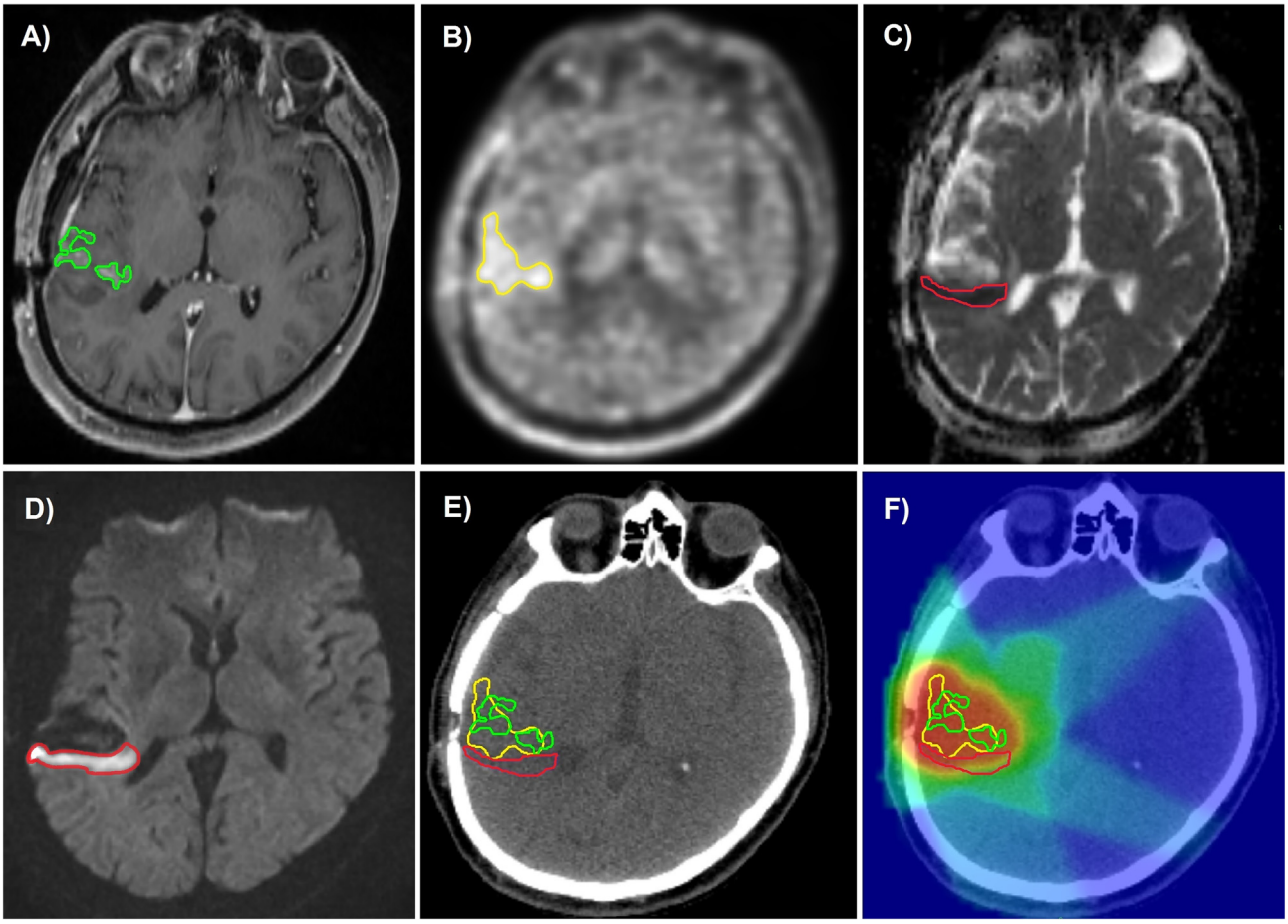

Fig. 3. Patient 27. A) Axial GdT1w-MRI, green: GTV-GdT1w-MRI. B) Axial FET-PET, yellow: GTV-PET. C) ADC map, red: GTV-ADClow, corresponding to a hyperintensity in D) DWI-MRI. E) Illustration of all three volumes on planning CT. F) Dose distribution of the treatment plan based on FET-PET.

(mean 2.39 ± 1.87 ml, median 1.68 ml, range 0.27–7.52 ml; $p < 0.0001$). GTV-PET measured on average 13.82 ± 11.91 ml (median 10.79 ml, range 0.36–46 ml), significantly larger than GTV-ADClow ($p < 0.0001$).

DSC values of 0.11 ± 0.09 between GTV-GdT1w-MRI and GTV-ADClow and 0.10 ± 0.09 between GTV-PET and GTV-ADClow further quantitatively described the only slight congruence of these volumes. DSC values between GTV-GdT1w-MRI and GTV-PET were comparatively higher, with a mean of 0.44 ± 0.2 (median 0.43, range 0.04–0.8).

The overlap volume between GTV-GdT1w-MRI and GTV-ADClow was on average 0.80 ± 0.85 ml (median 0.55 ml, range 0–3.25 ml), while the non-overlapping fraction was significantly larger (mean 1.60 ± 1.4 ml, median 1.15 ml, range 0.09–5.58 ml, $p = 0.009$). The overlap between GTV-PET and GTV-ADClow ranged between 0 and 3.21 ml with a median of 0.4 ml and a mean of 0.88 ± 0.98 ml. The non-overlapping sections measured on average 1.51 ± 1.28 ml (median 1.10 ml, range 0.19–4.85 ml) and were significantly larger than the overlapping areas ($p = 0.009$). The volumetric comparison thus revealed that the majority of the GTVs-ADClow is located outside areas of contrast enhancement in GdT1w-MRI (mean *non*-overlapping volume 66.2 ± 24.6%, median 72.2%, range 5.8–100%) and outside areas of increased FET-uptake (mean *non*-overlapping volume 76.4 ± 64%, median 69.5%, range 12.3–385.1%) (Figs. 2, 3 and Table A3 in Appendix A).

Commonly delineated volumes between GTV-ADClow and GTV-GdT1w-MRI (mean 0.32 ± 0.25, median 0.27, range 0–0.94) were not significantly different from the ones between GTV-ADClow and GTV-PET (mean 0.34 ± 0.26, median 0.34, range 0–0.87). Adjusting the planning volume by additionally taking into account restricted diffusion areas would thus imply a mean increase in GTV of up to 48.5% (SD 115.64%, median 24.64%, range 3.21–647.12%).

DVH analysis

For the 30 patients with restricted diffusion areas, all three GTVs were integrated in the DVH of the plan used for re-irradiation. The dose distribution in the volume chosen for treatment planning was homogenous and received the full prescribed dose. The GTV-ADClow volume receiving 95% of the dose (V95%) received 71.61 ± 30.54% of the dose prescribed to the PTV (median 79.65%, range 0–100%), while the volume receiving 80% of the dose (V80%) received 78.27 ± 26.69% of the prescription dose (median 92.05%, range 0–100 %). The mean dose in the GTVs-ADClow was 81.99 ± 28.12% (median 95.35%, range 0.9–107.4%), while the minimum was 52.52 ± 36.50% of the prescribed dose (median 47.80%, range 0.6–100.5%). The mean near-maximum absorbed dose (D2%, $D_{nearmax}$) was 93.70 ± 26.37% of the prescribed dose (median 102.65%, range 1–102.65%). Assuming a prescription of 39 Gy, the GTVs-ADClow would have received a mean dose of 31.97 ± 10.96 Gy, a minimum of 20.48 ± 14.23 Gy and a maximum of 36.54 ± 10.28 Gy. For the GTVs-ADClow we calculated a heterogeneity index (HI) of 0.58 ± 0.72 (median 0.36, range 0.02–2.97) and a conformity index (CI) of 42.26 ± 64.12 (median 18.3, range 0.75–277.9). More information on the DVH-parameters for the individual patients can be found in Appendix A. Examples of GTVs-ADClow and their dose coverage are shown in Figs. 4 and 5.

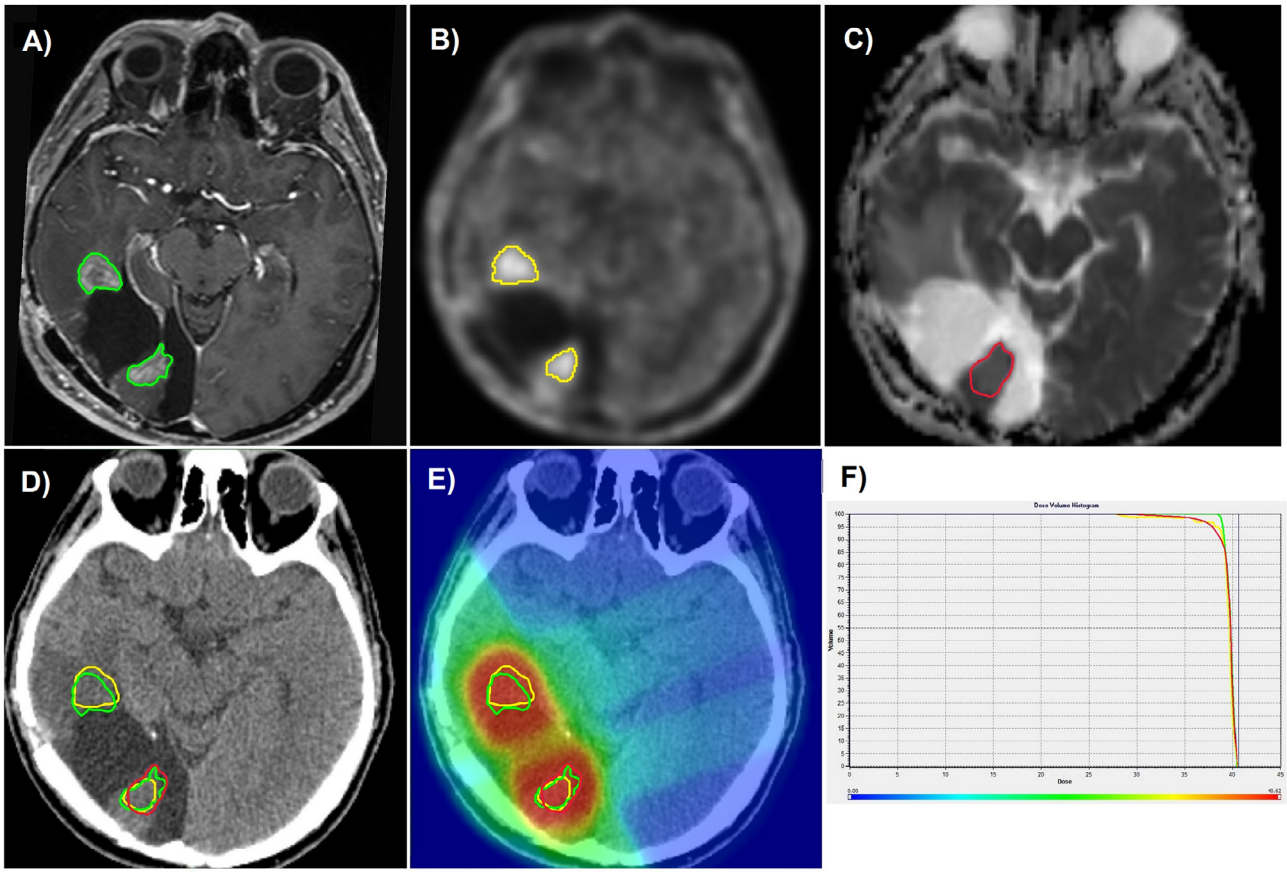

Fig. 4. Patient 1. A) Axial GdT1w-MRI, green: GTV-GdT1w-MRI. B) Axial FET-PET, yellow: GTV-PET. C) ADC map, red: GTV-ADClow. D) Illustration of all three volumes on planning CT. E) Dose distribution and F) DVH of the treatment plan based on GdT1w-MRI. All volumes show homogeneous and appropriate dose coverage.

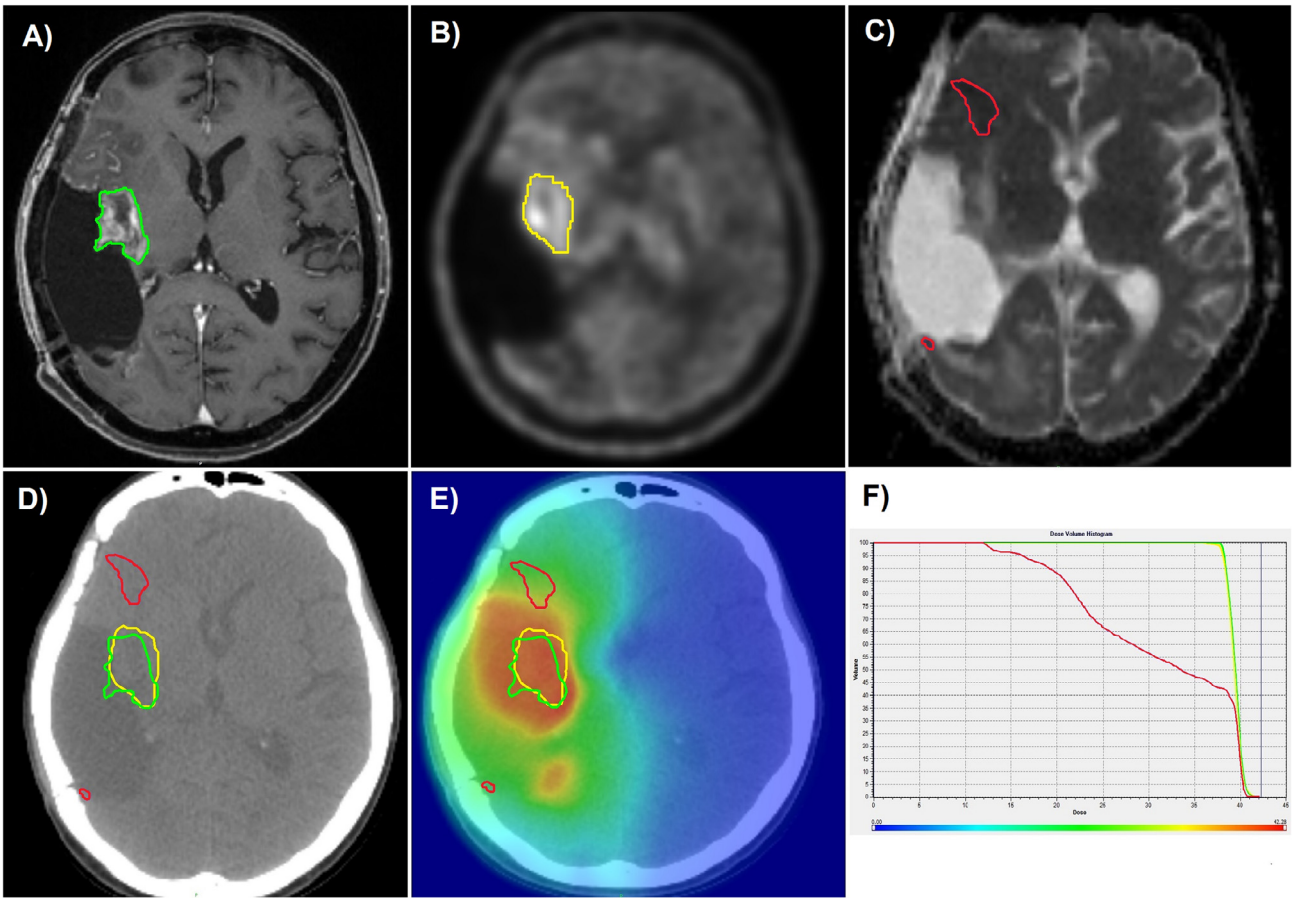

Fig. 5. Patient 6. A) Axial GdT1w-MRI, green: GTV-GdT1w-MRI. B) Axial FET-PET, yellow: GTV-PET. C) ADC map, red: GTV-ADClow. D) Illustration of all three volumes on planning CT. E) Dose distribution and F) DVH of the treatment plan based on GdT1w-MRI. GTV-GdT1w-MRI (green) and GTV-PET (yellow) show homogeneous and good dose coverage, while GTV-ADClow (red) shows significant underdosage.

Recurrence analysis

32 of 41 patients had a confirmed tumor progression on average 3.6 months (mean 3.6 ± 2, median 2.8, range 0.8–8.8 months) after re-irradiation. 23 of these 32 patients had restriction diffusion areas at baseline. Mean DSCs between GTV-R and GTV-ADClow (0.06 ± 0.05) were significantly lower than DSCs between GTV-R and GTV-GdT1w-MRI (0.28 ± 0.14, $p < 0.0001$) and lower than DSCs between GTV-R and GTV-PET (0.44 ± 0.78, $p = 0.047$, not statistically significant at a corrected α=0.025). DSCs between GTV-R and GTV-GdT1w-MRI and DSCs between GTV-R and GTV-PET were also not significantly different ($p = 0.255$). 91.3% of recurrent tumors involved in different proportions all three baseline-GTVs at once. In only three cases with multifocal recurrence, one volume exclusively predicted tumor progression in a certain region (in 1 case GTV-ADClow – Fig. 6, and in 2 cases GTV-GdT1w-MRI).

Discussion

In our study, we aimed to comparatively evaluate the information brought by FET-PET, GdT1w-MRI and ADC/DWI for GTV definition. To our knowledge, this is the first prospective trial assessing the differences between these imaging modalities in the re-irradiation treatment planning for rGBM.

In the cohort of 30 patients exhibiting a restricted diffusion, the volume of GTV-ADClow was the smallest of the three baseline GTVs, while GTV-PET was the largest. The difference in size and location between AA-PET and the GdT1w-MRI volumes was also previously observed in several studies [5,6,21]. In primary GBM, Niyazi et al. [21] similarly found significantly larger tumor volumes delineated according to FET-PET compared to the corresponding MRI-GTVs and substantial differences in location in the majority of patients.

Concerning the size and location of DWI/ADC in the radiation treatment planning of gliomas, there are only limited data available in the literature. In the current study, we used ADC maps and not DWI sequences for the delineation of GTVs-ADClow, so as to both allow for voxel-based quantitative analysis and avoid T2 shine-through effects. The small size may have resulted from filtering ADC reductions of other causes (infarction, etc.) by a careful analysis of the entire MRI data set. The mean ADC value in the defined ROIs was $0.74 \pm 0.22 \times 10^{-3}$ mm^2/s, thus situating the GTVs-ADClow in areas of definitely dense cellularity if compared with data acquired for primary GBM. Eidel et al. [15] found in 561 stereotactic biopsy primary GBM specimens a mean ADC value of $1.12 \pm 0.34 \times 10^{-3}$ mm^2/s at a mean cellularity of 3308.71 ± 1915.32 cells/mm^2 and an inverse correlation between the two. Furthermore, in a publication by Pramanik et al. [22] the presence of restricted diffusion areas in primary GBM correlated with a shorter progression-free survival and, more importantly, the insufficient dose coverage of these regions was considered a negative predictive factor. In comparison to our study, the authors did not use ADC maps or correlations with anatomical MR sequences for the GTV definition, which might have led to considerably larger volumes (median 9.8 ml, range 0.58–67 ml).

We also found that approximately 2/3 of the GTVs-ADClow were located outside the respective GTVs used for re-irradiation. This suggests that the target volume definition according to GdT1w-MRI and/or FET-PET may not cover the entire biologically

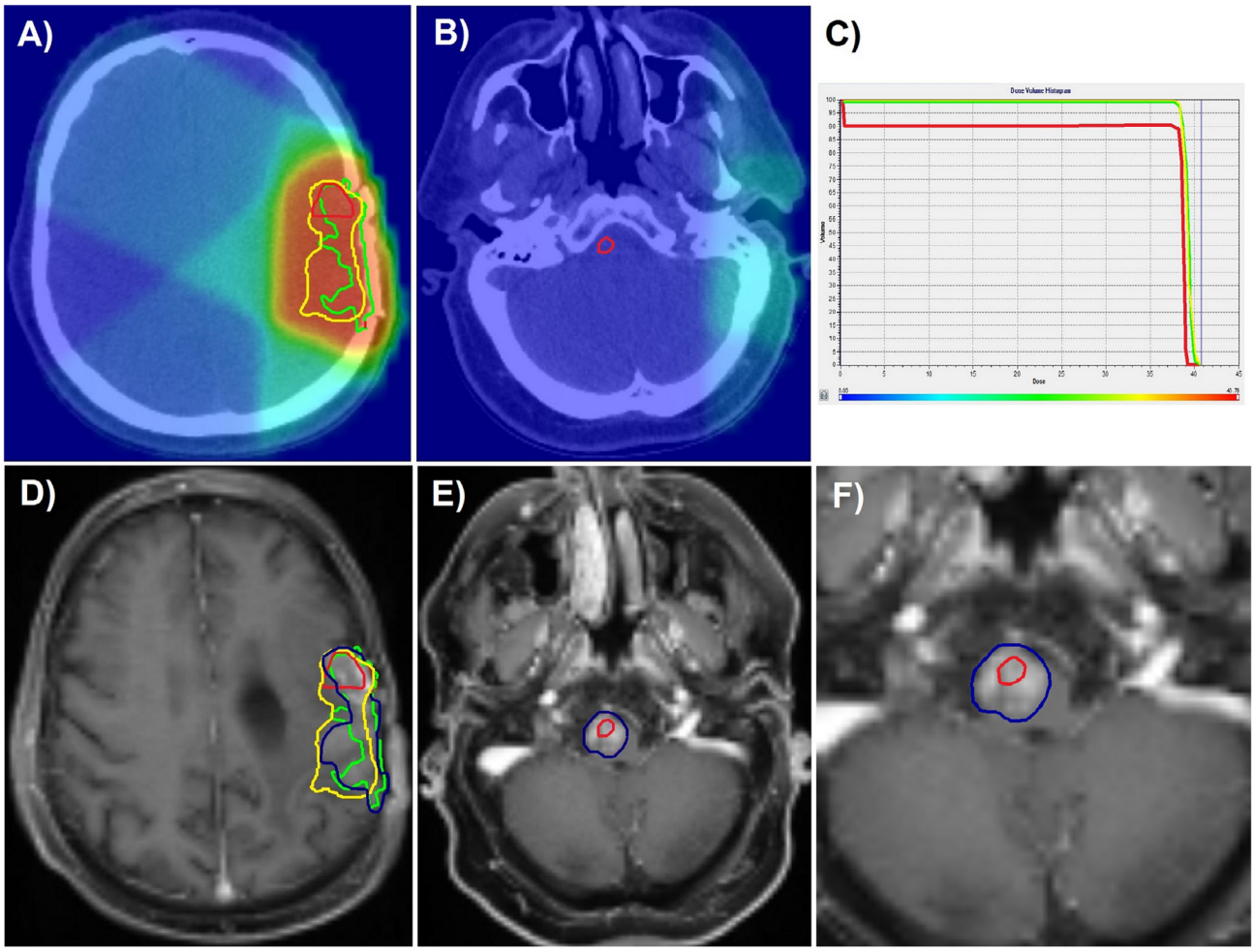

Fig. 6. Patient 33. A), B) Dose distribution and illustration of all three baseline volumes on the planning CT for re-irradiation treatment planning: GTV-GdT1w-MRI (green), GTV-PET (yellow), GTV-ADClow (red). C) DVH of the re-irradiation plan, GTV-ADClow (red) shows underdosage corresponding to the brainstem lesion. D) Confirmed recurrent tumor (blue) in pre-irradiated region and E) in brainstem, the latter emerging from previously identified but not treated area of restricted diffusion (red). F) Zoom in on the brainstem recurrent lesion (blue) centered by the baseline GTV-ADClow (red).

active tumor. The incongruence between GTV-ADClow and PET also indicates that the two investigations depict different underlying biological properties. This agrees with earlier studies comparing ADC and AA-PET in both low and high grade primary brain tumors [23,24]. These studies found only minimal anatomic overlap between the two and suggested that tissue compression and alteration of water distribution may play a more significant role in ADC than tumor cell density. Exploring whether the one or the other investigation really corresponds to active tumor tissue in rGBM is warranted and necessitates the direct comparison with pathologic findings as diagnostic gold standard. Pauleit et al. [25] explored the histopathologic correlation of ADC in 22 primary GBM patients and found a significantly lower ADC lesion-to-brain ratio in tumor compared to peritumoral tissue, though without significant predictive value.

Evaluated by DVH, the GTVs-ADClow were in our cohort only partially included in the high dose volume, but still received a median of 95% of the prescribed dose. This implies a relative spatial proximity, especially to the GdT1w-MRI volumes. Mean values for HI and CI supported the fact that the dose coverage in the GTVs-ADClow was less homogeneous and less conformal.

Nevertheless, the evaluation of relapse patterns revealed that recurrences more often derived from baseline GdT1w-MRI- and PET- rather than from ADC-volumes. Similarly, Khalifa et al. [26] found in a prospective analysis of 15 primary GBM patients that diffusion-restricted areas could not predict relapse sites. Even though recurrences were in our study exclusively delineated on follow-up GdT1w-MRI, which would potentially represent a bias in favor of this method, the correlation of recurrent tumors with baseline GTV-PET appeared, though non-significantly, to be the highest. This is comparable with results of Tsien et al. [27], who showed a correlation between MET-PET and regions of high risk of recurrence not defined by MRI in primary GBM. Galldicks et al. [28] also found significant FET-uptake differences between real tumor recurrence and pseudoprogression, while previous MRI-based studies have failed to do so [29]. All in all, our results regarding FET-PET/CT are in accordance with the current RANO (Response Assessment in Neuro-Oncology) and EANO (European Association for Neuro-Oncology) recommendations and further suggest that FET-PET may help delineate tumor extent not only in newly diagnosed GBM, but also in rGBM [30].

A limitation of the current study is the fact that the GTVs-ADClow were manually drawn. Thus, the ROI location, number and size were operator-dependent and could have led to a selection bias and a lower reproducibility, as described before [31]. To minimize these, we ensured that GTVs-ADClow were delineated by two independent investigators. Although no ADC threshold was defined, the very low mean values support the ROI selection. A further limitation is the reduced spatial resolution of ADC maps and their different voxel size compared to the GdT1w-MRI sequences, leading upon their co-

registration to an interpolation of ADC values. Furthermore, DWI is prone to geometrical distortions. However, especially in the echo-planar imaging-sequences used for ADC measurements, distortions are mainly due to the field inhomogeneity caused by the patient's presence itself and are locally small. Moreover, as recent studies have shown, there should be hardly any intra- and cross-system variations to be expected in the measurement of ADC values [32]. Another source of bias could be the co-registration itself. This was minimized through high precision automatic CT/PET image fusion, as described by Grosu et al. [33], and rigid mutual information fusion of MRI images, followed by a thorough verification and manual adjustment according to anatomical landmarks.

In this study we showed that areas of restricted diffusion on ADC/DWI do not correlate well with regions of either increased FET uptake or GdT1w-MRI contrast enhancement for the re-irradiation treatment planning of rGBM. We also highlighted that GTV-GdT1w-MRI and GTV-PET in rGBM only match in a proportion of 44%, supporting ongoing clinical studies on this matter, such as the GLIAA trial [11]. Surprisingly, GTV-ADClow was often localized outside both GTV-PET and GTV-GdT1w-MRI. From the radiation oncologist's point of view, a higher tumor cell density would require a dose escalation. Considering that restricted diffusion correlates with hypercellularity, the relevance of this volume discrepancy has to be further investigated in histopathological studies.

Funding/Acknowledgements

Financial support was provided by the *Deutsche Krebshilfe* Foundation, Germany (grant ID 111141) and German Cancer Consortium (DKTK), Germany (no grant ID available). We would also like to thank the Else Kröner-Fresenius Foundation, Germany, for the partial funding of Dr. Ilinca Popp within the EXCEL (Excellent Clinician Scientists in Freiburg – Education for Leadership) Programme "Immunological Causes and Therapies of Cancer". The funding sources had no involvement in the study design, in the collection, analysis and interpretation of data, in the writing of the report or in the decision to submit the article for publication.

Conflicts of interest

None.

Appendix A

Tables A1–A4.

Table A1
Patient characteristics.

Age	
Median	58
Range	35–77
Sex	
Men – no. (percentage)	31 (76%)
Women – no. (percentage)	10 (24%)
ECOG Performance Status	
0	16
1	25
Location of recurrent tumor (more than 1 location/patient possible)	
More than one lobe involved	23
Frontal lobe	19
Temporal lobe	27
Parietal lobe	13
Occipital lobe	7
Corpus callosum	1
IDH mutational status	
mutated	3
wild type	31
unknown	7
MGMT promoter methylation status	
methylated	7
not methylated	11
unknown	23

Table A2
ADC-values of ADClow ROIs.

Patient no.	ADC1 mm^2/s	ADC2 mm^2/s	ADC3 mm^2/s	ADC4 mm^2/s	ADC5 mm^2/s	ADC6 mm^2/s	ADC7 mm^2/s
1	0.75	1.16	0.84				
2	0.66	0.56	0.75	1.18			
3	0.71	0.98	0.73				
6	0.77	0.67	0.56	0.51	0.58	0.72	0.60
7	0.90	0.86	0.86				
8	0.98						
9	0.97	0.96	1.02	0.67			
11	0.61	0.59	0.48	0.58	0.47	0.64	0.45
12	0.92	0.95	0.91	0.87	0.80	0.63	
13	0.25	0.52	0.62	0.5	0.54	0.68	
15	0.56	1.21	0.94	1.05			
16	0.82	0.45					
17	0.85	0.81	0.78				

Table A2 (*continued*)

Patient no.	ADC1 mm^2/s	ADC2 mm^2/s	ADC3 mm^2/s	ADC4 mm^2/s	ADC5 mm^2/s	ADC6 mm^2/s	ADC7 mm^2/s
18	0.68	0.85					
21	1.09	0.98	0.99				
23	0.65	0.61	0.87	0.68			
24	0.57	0.60	0.6	0.57			
25	0.80	0.76	0.90				
26	1.44	1.01					
27	0.31	0.35	0.28	0.46	0.39	0.43	
28	0.89	0.66	0.93	1.10			
30	0.57						
32	0.69	0.79	1.09	0.82			
33	0.74	0.66	0.83				
36	0.59	0.7	0.42				
37	0.81	0.97	0.9				
38	0.89	0.76					
39	0.83	0.67	0.65				
40	0.62	0.46	0.77				
41	0.95	0.81					

Table A3
Volumetric comparison of GTVs-ADClow, GTVs-GdT1w-MRI and GTVs-PET.

Patient no.	GTV-GdT1w-MRI (ml)	GTV-PET (ml)	GTV-ADClow (ml)	Overlap (GdT1w-MRI, PET) (ml)	Overlap (ADClow, GdT1w-MRI) (ml)	Non-overlap (ADClow, GdT1w-MRI) (ml)	Overlap (ADClow, PET) (ml)	Non-overlap (ADClow, PET) (ml)	Union GTV (ADClow, GdT1w-MRI) (ml)	Union GTV (ADClow, PET) (ml)	CDV (ADClow, GdT1w-MRI)	CDV (ADClow, PET)	DSC (ADClow, GdT1w-MRI)	DSC (ADClow, PET)
1	8.60	6.66	5.30	4.75	2.73	2.57	1.84	3.45	11.18	10.11	0.52	0.35	0.39	0.31
2	3.05	1.86	1.44	0.72	0.28	1.16	0.16	1.27	4.21	3.13	0.19	0.11	0.12	0.10
3	14.62	15.01	1.32	10.61	0.96	0.36	0.78	0.54	14.98	15.54	0.73	0.59	0.12	0.10
4	1.77	2.06	–	0.59	–	–	–	–	–	–	–	–	–	–
5	4.76	2.93	–	1.13	–	–	–	–	–	–	–	–	–	–
6	13.49	11.92	2.86	8.24	0.61	2.25	0.00	2.86	15.76	14.77	0.21	0.00	0.07	0.00
7	48.27	45.71	1.55	23.03	1.45	0.09	1.35	0.19	48.37	46.29	0.94	0.87	0.06	0.06
8	5.75	14.78	0.27	5.74	0.00	0.27	0.00	0.27	6.02	15.05	0.00	0.00	0.00	0.00
9	22.38	25.58	6.52	17.59	3.25	3.27	3.21	3.31	25.65	28.89	0.50	0.49	0.22	0.20
10	11.43	10.34	–	8.75	–	–	–	–	–	–	–	–	–	–
11	16.68	27.85	3.89	14.23	2.20	1.69	2.90	0.99	18.36	28.95	0.57	0.75	0.21	0.18
12	12.77	13.24	7.52	10.14	1.93	5.58	2.67	4.85	18.35	18.09	0.26	0.36	0.19	0.26
13	3.03	0.36	3.01	0.23	0.06	2.96	0.00	3.01	5.99	3.38	0.02	0.00	0.02	0.00
14	5.95	4.35	-	2	–	–	–	–	–	–	–	–	–	–
15	3.18	1.53	2.62	0.93	0.62	2.00	0.54	2.08	5.18	3.61	0.24	0.21	0.21	0.26
16	13.93	9.40	1.54	4.98	0.48	1.06	0.39	1.14	14.99	10.55	0.31	0.25	0.06	0.07
17	7.11	9.50	1.85	5.27	1.04	0.81	1.38	0.46	7.92	9.96	0.56	0.75	0.23	0.24
18	19.14	46	1.36	16.99	0.19	1.17	0.19	1.17	20.31	49.02	0.14	0.14	0.02	0.01
19	1.35	0.68	–	0.31	–	–	–	–	–	–	–	–	–	–
20	5.40	13.93	–	4.56	–	–	–	–	–	–	–	–	–	–
21	13.61	12.72	1.81	7.83	0.67	1.14	0.18	1.63	14.75	14.35	0.37	0.10	0.09	0.02
22	5.13	5.84	–	4.13	–	–	–	–	–	–	–	–	-	-
23	11.33	21.66	2.94	4.15	1.63	1.31	2.13	0.81	12.64	22.47	0.55	0.72	0.23	0.17
24	3.43	4.40	0.39	0.56	0.05	0.34	0.11	0.28	3.77	4.68	0.13	0.28	0.03	0.05
25	0.95	2.60	0.61	0.68	0.05	0.56	0.20	0.41	1.51	3.01	0.08	0.33	0.06	0.12
26	21.61	8.04	1.17	6.05	0.22	0.95	0.12	1.06	22.56	9.10	0.19	0.10	0.02	0.03
2–7	12.10	9.96	4.23	2.99	1.23	3.01	0.14	4.09	15.10	14.05	0.29	0.03	0.15	0.02
28	0.87	31.45	5.63	0.59	0.23	5.4	2.82	2.81	6.27	34.26	0.04	0.50	0.07	0.15
29	28.68	24.16	–	10.8	–	–	–	–	–	–	–	-	-	-
30	21.47	10.94	0.86	0.71	0.10	0.76	0.34	0.52	22.23	11.45	0.12	0.40	0.01	0.06
31	1.13	2.14	-	1.01	-	-	-	-	-	-	-	-	-	-
32	8.31	10.79	2.69	4.33	0.91	1.78	1.15	1.54	10.10	12.32	0.34	0.43	0.17	0.17
33	15.20	32.00	2.17	11.75	1.28	0.89	1.64	0.53	16.09	32.53	0.59	0.76	0.15	0.10
3–4	4.03	8.27	–	3.58	–	–	–	–	–	–	–	–	–	–
35	4.20	16.93	–	4.08	–	–	–	–	–	–	–	–	–	–
36	22.08	14.20	1.50	10.01	0.76	0.74	0.16	1.34	22.82	15.54	0.51	0.11	0.06	0.02
37	11.60	27.46	3.46	4.8	0.49	2.97	0.90	2.56	14.57	30.02	0.14	0.26	0.07	0.06
38	6.29	36.68	0.60	4.89	0.16	0.44	0.41	0.19	6.73	36.87	0.27	0.68	0.05	0.02
39	2.59	11.57	0.71	1.49	0.02	0.69	0.01	0.70	3.28	12.27	0.03	0.01	0.01	0.00
40	6.12	4.47	0.62	2.73	0.44	0.18	0.22	0.40	6.31	4.88	0.71	0.35	0.13	0.09
41	4.25	6.59	1.48	1.42	0.03	1.45	0.56	0.92	5.70	7.51	0.02	0.38	0.01	0.14
Mean	10.43	13.82	2.39	5.59	0.80	1.60	0.88	1.51	13.39	17.42	0.32	0.34	0.11	0.10
SD	9.34	11.91	1.87	5.36	0.85	1.40	0.98	1.28	9.46	12.57	0.25	0.26	0.09	0.09
Median	7.11	10.79	1.68	4.33	0.55	1.15	0.40	1.10	13.61	14.20	0.27	0.34	0.07	0.08
Range	0.87–48.27	0.36–46	0.27–7.52	0.23–23.03	0.00–3.25	0.09–5.58	0.00–3.21	0.19–4.85	1.51–48.37	3.01–49.02	0.00–0.94	0.00–0.87	0.00–0.39	0.00–0.31

Table A4
DVH-Analysis for GTV-ADClow.

Patient no.	V95%	V80%	D_{MIN} %	D_{MEAN} %	$D_{NEARMAX}$ %	HI	CI
1	97	99.6	65.67	101.6	103.85	0.11	4.35
2	86	93.1	40.2	98.9	106.2	0.49	17.8
3	99.5	100	92.6	99.3	104	0.07	11.14
6	43.7	54.2	30.6	79.9	103.8	0.83	9.41
7	77.9	100	91	95.9	100.5	0.1	5.26
8	0	0	0.8	0.9	1	0.25	80.09
9	67.9	75.7	38.9	90.1	102.9	0.51	6.5
11	97.6	100	93.9	99.7	104	0.09	12.2
12	54.2	63.9	9.8	32.6	40.5	0.72	3
13	0	0	2.2	12.7	32.7	2.6	1
15	79.6	79.5	15.1	86.8	102.4	0.81	5.6
16	94.4	100	81.4	100.2	102.3	0.12	18.8
17	99	100	93.9	99.3	104	0.09	7.69
18	17.6	26.1	17.2	56	101.3	1.7	52.6
21	79.7	94.2	66.5	97.1	102.3	0.28	0.75
23	100	100	97.7	102.3	107.1	0.09	26.6
24	100	100	96.6	103	105.3	0.08	199.1
25	36	35.9	17.4	51	99.3	2.97	100.1
26	100	100	98.4	99.7	100.7	0.02	277.9
27	21.7	59.1	33.08	81	100.1	0.62	2.6
28	53.7	55.3	1.4	58.9	101	1.01	8.2
30	66	98	31.11	43.6	45.5	0.2	58.6
32	89.6	100	86.34	97.8	101.1	0.13	2.8
33	91	91	0.6	90.5	100.6	1.01	23.6
36	100	100	100	101	102.9	0.02	51.7
37	79.6	88.2	21.2	94.8	106	0.76	23.86
38	100	100	100.5	107.4	109.5	0.06	151.1
39	63.9	63.9	58.5	89	103.9	0.43	60.1
40	72.9	81.4	37.6	90.8	108.8	0.69	19.4
41	79.9	89.1	55.4	97.8	107.5	0.51	25.9

References

[1] Nieder C, Astner ST, Mehta MP, et al. Improvement, clinical course, and quality of life after palliative radiotherapy for recurrent glioblastoma. Am J Clin Oncol 2008;31(3):300–5.
[2] Nieder C, Adam M, Molls M, et al. Therapeutic options for recurrent high-grade glioma in adult patients: recent advances. Crit Rev Oncol Hematol 2006;60(3):181–93.
[3] Verma N, Cowperthwaite MC, Burnett MG, et al. Differentiating tumor recurrence from treatment necrosis: a review of neuro-oncologic imaging strategies. Neuro-Oncol 2013;15(5):515–34.
[4] Rachinger W, Goetz C, Pöpperl G, et al. Positron emission tomography with O-(2-[18F]fluoroethyl)-l-tyrosine versus magnetic resonance imaging in the diagnosis of recurrent gliomas. Neurosurgery 2005;57(3):505–11.
[5] Grosu AL, Weber WA, Franz M, et al. Reirradiation of recurrent high-grade gliomas using amino acid PET (SPECT)/CT/MRI image fusion to determine gross tumor volume for stereotactic fractionated radiotherapy. Int J Radiat Oncol Biol Phys 2005;63(2):511–9.
[6] Grosu A-L, Weber WA, Riedel E, et al. L-(methyl-11C) methionine positron emission tomography for target delineation in resected high-grade gliomas before radiotherapy. Int J Radiat Oncol Biol Phys 2005;63(1):64–74.
[7] Pauleit D, Floeth F, Hamacher K, et al. O-(2-[18F]fluoroethyl)-L-tyrosine PET combined with MRI improves the diagnostic assessment of cerebral gliomas. Brain 2005;128(Pt 3):678–87.
[8] Weber WA, Grosu AL, Czernin J. Technology Insight: advances in molecular imaging and an appraisal of PET/CT scanning. Nat Clin Pract Oncol 2008;5(3):160–70.
[9] Grosu A-L, Weber WA. PET for radiation treatment planning of brain tumours. Radiother Oncol 2010;96(3):325–7.
[10] Grosu A-L, Astner ST, Riedel E, et al. An interindividual comparison of O-(2-[18F]fluoroethyl)-L-tyrosine (FET)- and L-[methyl-11C]methionine (MET)-PET in patients with brain gliomas and metastases. Int J Radiat Oncol Biol Phys 2011;81(4):1049–58.
[11] Oehlke O, Mix M, Graf E, et al. Amino-acid PET versus MRI guided re-irradiation in patients with recurrent glioblastoma multiforme (GLIAA) – protocol of a randomized phase II trial (NOA 10/ARO 2013-1). BMC Cancer 2016;16(1):769.
[12] Hutterer M, Nowosielski M, Putzer D, et al. [18F]-fluoro-ethyl-L-tyrosine PET: a valuable diagnostic tool in neuro-oncology, but not all that glitters is glioma. Neuro-Oncol 2013;15(3):341–51.
[13] Pöpperl G, Götz C, Rachinger W, et al. Value of O-(2-[18F]fluoroethyl)-l-tyrosine PET for the diagnosis of recurrent glioma. Eur J Nucl Med Mol Imaging 2004;31(11):1464–70.
[14] Surov A, Meyer HJ, Wienke A. Correlation between apparent diffusion coefficient (ADC) and cellularity is different in several tumors: a meta-analysis. Oncotarget 2017;8(35):59492–9.
[15] Eidel O, Neumann J-O, Burth S, et al. Automatic analysis of cellularity in glioblastoma and correlation with ADC using trajectory analysis and automatic nuclei counting. PLoS One 2016;11(7):e0160250.
[16] Tsien C, Cao Y, Chenevert T. Clinical applications for diffusion magnetic resonance imaging in radiotherapy. Semin Radiat Oncol 2014;24(3):218–26.
[17] Cha J, Kim ST, Kim H-J, et al. Differentiation of tumor progression from pseudoprogression in patients with posttreatment glioblastoma using multiparametric histogram analysis. Am J Neuroradiol 2014;35(7):1309–17.
[18] Tien RD, Felsberg GJ, Friedman H, et al. MR imaging of high-grade cerebral gliomas: value of diffusion-weighted echoplanar pulse sequences. Am J Roentgenol 1994;162(3):671–7.
[19] Asao C, Korogi Y, Kitajima M, et al. Diffusion-weighted imaging of radiation-induced brain injury for differentiation from tumor recurrence. Am J Neuroradiol 2005;26(6):1455–60.
[20] Grégoire V, Mackie TR. State of the art on dose prescription, reporting and recording in Intensity-Modulated Radiation Therapy (ICRU report No. 83). Cancer Radiother 2011;15(6–7):555–9.
[21] Niyazi M, Geisler J, Siefert A, et al. FET-PET for malignant glioma treatment planning. Radiother Oncol 2011;99(1):44–8.
[22] Pramanik PP, Parmar HA, Mammoser AG, et al. Hypercellularity components of glioblastoma identified by high b-value diffusion-weighted imaging. Int J Radiat Oncol Biol Phys 2015;92(4):811–9.
[23] Rose S, Fay M, Thomas P, Bourgeat P, et al. Correlation of MRI-derived apparent diffusion coefficients in newly diagnosed gliomas with [18F]-fluoro-L-dopa PET: what are we really measuring with minimum ADC? AJNR Am J Neuroradiol. 2013;34(4):758–64.
[24] Rahm V, Boxheimer L, Bruehlmeier M, et al. Focal changes in diffusivity on apparent diffusion coefficient MR imaging and amino acid uptake on PET do not colocalize in nonenhancing low-grade gliomas. J Nucl Med. 2014;55(4):546–50.
[25] Pauleit D, Langen KJ, Floeth F, et al. Can the apparent diffusion coefficient be used as a noninvasive parameter to distinguish tumor tissue from peritumoral tissue in cerebral gliomas? J Magn Reson Imaging. 2004;20(5):758–64.
[26] Khalifa J, Tensaouti F, Lotterie JA, et al. Do perfusion and diffusion MRI predict glioblastoma relapse sites following chemoradiation? J Neurooncol 2016;130(1):181–92.
[27] Tsien CI, Brown D, Normolle D, et al. Concurrent temozolomide and dose-escalated intensity-modulated radiation therapy in newly diagnosed glioblastoma. Clin Cancer Res 2012;18(1):273–9.
[28] Galldiks N, Dunkl V, Stoffels G, et al. Diagnosis of pseudoprogression in patients with glioblastoma using O-(2-[18F]fluoroethyl)-L-tyrosine PET. Eur J Nucl Med Mol Imaging 2015;42(5):685–95.
[29] Young RJ, Gupta A, Shah AD, et al. Potential utility of conventional MRI signs in diagnosing pseudoprogression in glioblastoma. Neurology 2011;76:1918–24.
[30] Albert NL, Weller M, Suchorska B, et al. Response Assessment in Neuro-Oncology working group and European Association for Neuro-Oncology

recommendations for the clinical use of PET imaging in gliomas. Neuro Oncol 2016;18(9):1199–208.
[31] Bilgili Y, Unal B. Effect of region of interest on interobserver variance in apparent diffusion coefficient measures. Am J Neuroradiol 2004;25(1):108–11.
[32] Jacobs MA, Malyarenko DI, Newitt DC, et al. Multisite Reproducibility of radiomics and ADC measurements for temperature-controlled phantom: Preliminary results. In: International society for magnetic resonance in medicine (ISMRM), 16-21.06.2018, Paris.
[33] Grosu AL, Lachner R, Wiedenmann N, et al. Validation of a method for automatic image fusion (BrainLAB System) of CT data and 11C-methionine-PET data for stereotactic radiotherapy using a LINAC: first clinical experience. Int J Radiat Oncol Biol Phys 2003;56(5):1450–63.